17th Australasian Fluid Mechanics Conference
Auckland, New Zealand
5-9 December 2010

Three-dimensional Numerical Simulation of Hydrodynamic Forces on an Oblique Cylinder in Oscillatory Flow

M. Zhao and L. Cheng

School of Civil and Resource Engineering
The University of Western Australia, 35 Stirling Highway, Crawley, WA 6009, Australia

Abstract

Sinusoidal oscillating flow around a circular cylinder at an oblique angle is investigated by direct numerical simulation. Simulations are carried out for oblique angles of α = 0°, 15°, 30°, 45° and 60°, Reynolds number Re = 2000 and KC number ranging from 6.75 to 30. The oblique angle is defined as the angle between the flow direction and the transverse plane of the cylinder (see Fig. 1). The predicted vortex shedding regimes agree well with those found from physical experiments. When the KC number is close to the boundary value of KC number between two vortex shedding regimes (KC = 6.75, 15, 20 and 30) the correlation of sectional force in cylinder's spanwise direction is very weak and the time series of the transverse force contains two or three predominant frequencies, implying the flow switches from one mode to another continuously. The span-wise correlation factor obtained according to the sectional transverse force is always close to 1 for single-mode flows. Comparison between the numerical results of α=0° and those of $\alpha\neq$0° shows that the independent principle is applicable for the calculated KC number range and the oblique angle ($\alpha\leq$60°). The oblique angle has little effect on mode-averaged transverse force and the in-line force coefficients.

Introduction

The study of oscillatory flow past a circular is of importance in offshore engineering because is represents wave impact on sub-sea cylindrical structures such as pipelines and risers. Extensive study has been done about oscillatory flow past a circular cylinder due to its engineering importance. Hydrodynamic forces and flow characteristics around a circular cylinder in a sinusoidal oscillatory flow are dependent on the Keulegan-Carpenter (KC) number and the Reynolds number. The KC number is defined as KC = $U_m T/D$, where U_m is the velocity amplitude of the oscillatory flow, T is the oscillatory period and D is the diameter of the cylinder. The Reynolds number is defined as Re = $U_m D/\nu$, where ν is the fluid kinematic viscosity. Oscillatory flow around a circular cylinder is classified into the pairing of attached vortices (0 < KC < 7), single pair (7 < KC < 15), double pair (15 < KC < 24), three pairs (24 < KC < 32) and four pairs (32 < KC < 40) vortex shedding regimes, based on the number of vortex pairs shed during each half of a flow period [1]. It was also found that the relationship between vortex motions and time-dependent lift-force variations in each vortex shedding regime. Obasaju [2] measured and analysed hydrodynamic forces on a circular cylinder undergoing sinusoidal motion in still water for KC ranging from 4 to 55 by a mode-averaging technique. It was reported that the span-wise correlation of vortex shedding does not decrease monotonically with increasing KC. The correlation is high when KC is close to the mid range of KC values of a vortex regime and low when KC is close to the two boundary KC values of a vortex shedding regime.

Although 2D models have revealed some fundamental features of the flow, some inherent characteristics of the flow can only be simulated by a three-dimensional (3D) model. Three-dimensional numerical studies show that three-dimensionality in the flow field always appears once the asymmetric vortex pattern is fully developed [3-5]. Studies about steady flow past a circular cylinder at an oblique attack showed that both the force coefficients and the vortex shedding frequency, that are normalized by the velocity component perpendicular to the cylinder, are approximately independent on the oblique angle [5-9]. This is often called the independence principle or the cosine law in literature. When an oscillatory flow past a cylinder at an oblique angle is concerned, the following questions may arise: (a) If a specific vortex shedding regime still happens in the same range of KC number as that in the right attack angle case; (b) If the independent principle applies to the oscillatory flow case. So far, to the best of our knowledge, no work has been done with regard to oscillatory flow around an oblique cylinder.

In this study, sinusoidal oscillatory flow past a circular cylinder at an oblique attack is investigated by direction numerical simulation. Three-dimensional Navier-Stokes equations are solved using a Petrov-Galerkin finite element method. In the present study the Reynolds number is a constant of 2000, the KC number ranges from 6.75 to 30. The flow oblique angles examined are 0°, 15°, 30°, 45° and 60°.

Numerical Method

Figure 1 shows the definition of the non-dimensional computational domain and the coordinate system. The velocity component in the y-direction is zero. The angle between the flow direction and the xy-plane is α. Three-dimensional quantities are non-dimensionalized by the cylinder diameter (D) and the amplitude of the oscillatory velocity in x-direction (U_m) as

$$x_i = x_i'/D,\ \ u_i = u_i'/U_m,\ \ p = p'/\rho U_m^2,\ \ t = t'/T,$$
$$\mathrm{Re} = U_m D/\nu,\ \ KC = U_m T/D, \tag{1}$$

where primes are used to denote dimensional variables, (x_1, x_2, x_3)=(x, y, z), u_i is the velocity component in the x_i-direction, ν is the kinematic viscosity, p is the pressure, T is the period of the oscillatory flow. The non-dimensional Navier-Stokes equations are

$$\frac{1}{KC}\frac{\partial u_i}{\partial t} + u_j\frac{\partial u_i}{\partial x_j} + \frac{\partial p}{\partial x_i} - \frac{1}{\mathrm{Re}}\frac{\partial^2 u_i}{\partial x_j^2} = 0, \tag{2}$$

$$\frac{\partial u_i}{\partial x_i} = 0. \tag{3}$$

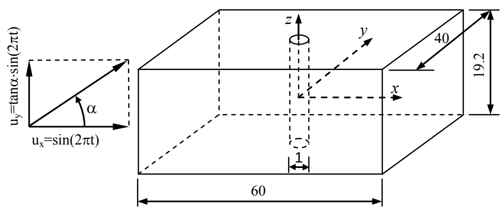

Figure 1. Computational domain in non-dimensional sizes

In the present study, flow past a circular cylinder of a length of 19.2 is studied. The governing equations were solved by a Petrov-Galerkin finite element model developed by Zhao et al. [9]. The boundary conditions for the governing equations are as follows:

At the left and right boundaries of the computational domain, the velocity is given by

$$(u_1,\ u_2,\ u_3) = (1,\ 0,\ \tan\alpha)\sin(2\pi t), \tag{4}$$

and the pressure gradient in the x-direction is $\partial p/\partial x = (2\pi/KC)\cos(2\pi t)$. At the two side boundaries that are parallel to the xz plane, the velocity component and the pressure gradient perpendicular to the boundary are zero. A periodic condition was imposed by setting velocity and pressure gradients (in all three directions) at the top and the bottom boundaries to be equal to each other. At the cylinder surface the no-slip boundary condition is applied.

The computational domain (60×40×19.2) was divided into hexahedron 8-node tri-linear elements. Figure 2 shows a typical computational mesh near the cylinder. The total number of nodal points is 1,203,840. The element size in the cylinder span-wise direction is 0.1. The node number along the circumference of a cross section of the cylinder surface is 80. The non-dimensional distance of a nodal point to the wall: $y^+=u_{fm}\Delta/\nu$, where Δ is the distance from the wall and u_{fm} is the maximum friction velocity, was less than 0.4 for all values of α and at least two layers of grid points were located within $y^+<1$. Mesh dependency study was done and it was demonstrated that further reducing mesh size make negligible difference on the results.

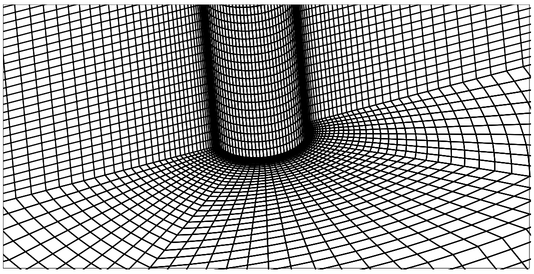

Figure 2. Typical computational mesh near the cylinder

Right attack angle (α=0°)

The numerical results shows that flow is in one pair regime for KC=10 and 13, where one vortex is shed in half flow period. Flows for KC=17.5 and 26.2 are in two- and three-pair regimes respectively. Figure 3(a-f) shows the contours of span-wise vorticity (ω_z) at six instants in xy-plane of z=0 within 20th cycle for α=0° and KC=17.5. The flow at this KC number is in two-pair retime. The instants P1 – P6 are defined in the Figure 3 (g) of time series of lift coefficient. When flow is in positive x-direction, two vortices are shed from the cylinder (Vortex A in P2 and Vortex B in P3). Instead of being shed from the cylinder surface, Vortex C generated in P3 go around the cylinder surface to the top side of the cylinder (P4) after flow reverse. The vortex street in the first half of a cycle points to the bottom right direction of the cylinder, while it points to the top left direction in the second half of the cycle, forming so-called diagonal vortex street.

Figure 4 shows the iso-surfaces of span-wise vorticity $|\omega_z|$=1.5 corresponding to the three instants indicated in Figure 3 (a-c). The span-wise vorticity is defined as $\omega_z = \partial v/\partial x - \partial u/\partial y$. A large incline angle between the vortex tube and the cylinder's span-wise direction is observed. The reason for this large incline angle is that there is a phase difference in the vortex shedding processes at different z-locations. The phase difference of the vortex shedding induces the phase variation of the fluctuating lift force in the span-wise direction. Flow regimes for other KC number are also observed in the numerical results and are not presented here due to paper limitation.

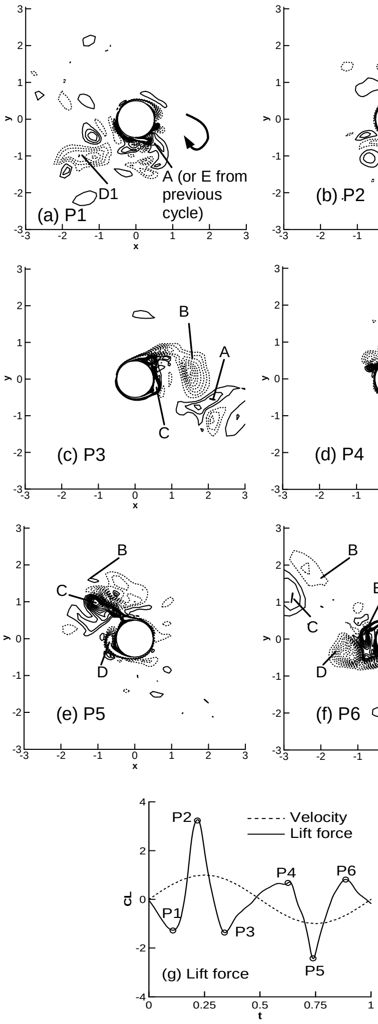

Figure 3. Contours of span-wise vorticity (ω_z) at four instants in 20th cycle; α=0°, KC=17.5 and z=0

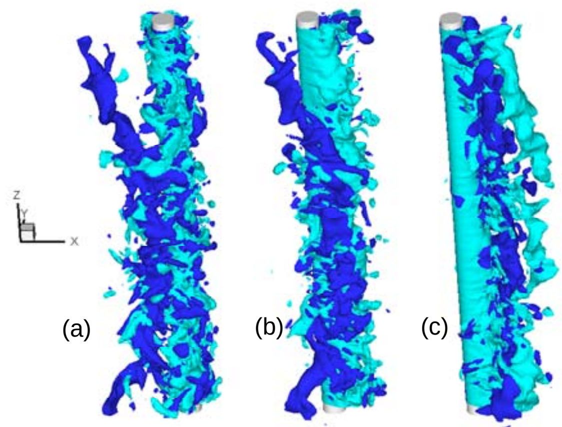

Figure 4. Iso-surface of span-wise vorticity Contours of $|\omega_z|$=1.5 at four instants in 20th cycle (the phases corresponds to those in Figure 3 (a-c)); α=0° and KC=17.5.

Oblique attack angle

When oscillatory flow past a circular at oblique attack angles is investigated, the amplitude of non-dimensional velocity component in the direction normal to the cylinder is kept to be 1. The Reynolds number, defined using the normal velocity component, is Re=2000. The KC number, defined by the maximum velocity in the direction perpendicular to the cylinder, are the same as those used for α=0°. The independence principle (or the cosine law) assumes that the hydrodynamic forces on the cylinder in the x- and y-directions can be modelled by the flow past a circular cylinder at right attack angle with the input velocity being the velocity component perpendicular to the cylinder span [10]. The validity of the independence principle, that was derived based on the case of steady currents, has not yet been verified and will be examined in the case of oscillatory flow.

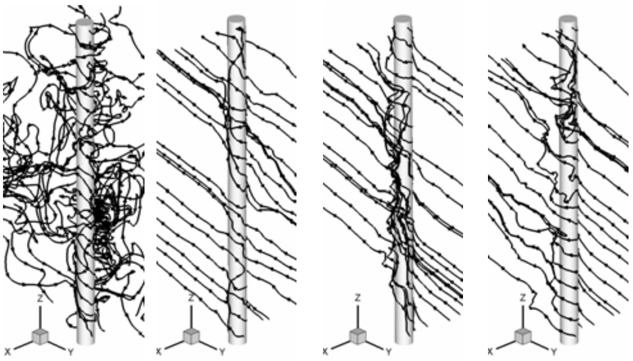

(a) t = 18 (b) t = 18.125 (c) t = 18.375 (d) t = 18.5

Figure 5. Streamlines for α=45°, KC=20

Figure 5 shows the streamlines around the cylinder for α=45°, KC=20 in four instants within a half of a flow period. When flow reverses at t=18, the streamlines is chaotic, indicating strong turbulence. It can be seen that the directions of the streamlines are altered significantly close to the cylinder. Some streamlines near the cylinder go in the span-wise direction in helical tracks as shown Figure 5 (b - d). These streamlines are found to be close to the centres of vortex tubes. In Figure 5 (c) and (d), the vortices move to the side of the cylinder. Correspondingly, the helical streamlines appear at the side of the cylinder too. Zhao et al. [9] also reported the helical streamlines near the cores of span-wise wake vortices in their study of steady flow past a circular cylinder at an oblique attack angle. In the oscillatory flow, the span-wise vortices may be located at any locations and the helical streamlines may appear wherever the vortices are located. In the next half-period of the flow those streamlines will reverse to the negative z-direction.

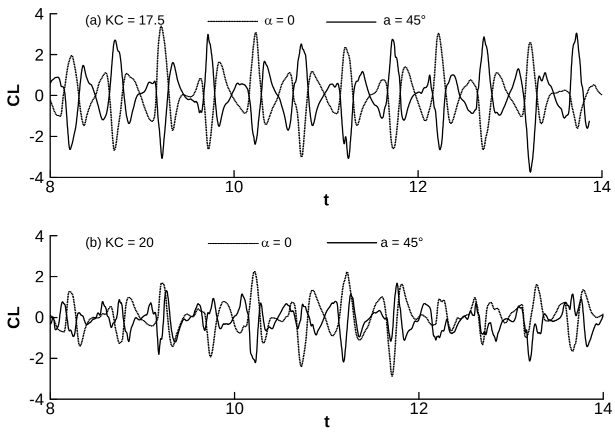

Figure 6. Comparison of the lift force between α=0° and α=45°

The forces on the cylinder at the oblique attack angle case are normalized by the velocity amplitude in the normal direction of the cylinder. Figure 6 shows the comparison of the time series of the lift force between α=0° and 45°. At KC = 17.5, the lift for α=45° is almost the mirror image of that for α=0°. At KC = 20, where the flow is in multi-frequency mode, both lift coefficients are highly irregular and no similarity between the lift coefficients can be found. The lift for α=45°appears to have high frequency wiggles compared to that of right attack angle case. However, it will be demonstrated later on that the mode averaged forces for two α values agree with each other.

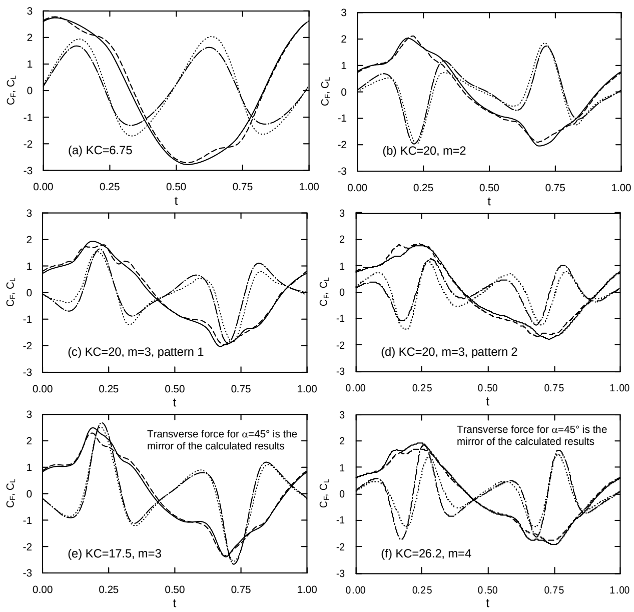

Figure 7. Comparion of mode-averaged force between α=0° and α=45°; ———, in-line α=0°; – – – – –, in-line α=45°; —·—·—, transverse α=0°; ··········· , transverse α=45°

The mode-averaging technique proposed in Reference [2] is employed to analyse the lift force on the cylinder. The mode-averaged forces for α=45° are compared with those for α=0° in Figure 7. In some cases of KC, at which the transverse forces at the two oblique angles are in anti-phase to each other, the mirror images of the transverse force for α=45° are plotted for the purpose of comparison. It can be seen that the mode averaged forces for the two attack angles agree with each other exceptionally well. Even when the flow is in multi-mode, the forces for each mode at α=45° agree well with its counterparts at α=0°. The vortex shedding regime at xy-plane is found to be independent on α also. The results of the vortex shedding patterns are not given due to the page limitation of the paper.

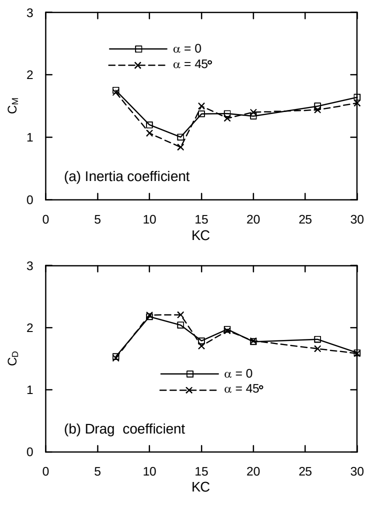

Figure 8. Comparison of in-line force coefficient between α=0° and α=45°

The Morison equation is usually used to describe the in-line force in the flow direction. The Morison equation is defined by

$$F_x = \frac{1}{4}\rho\pi D^2 C_M \frac{du(t)}{dt} + \frac{1}{2}\rho D C_D |u(t)|u(t) \tag{8}$$

where u(t) is the free-stream velocity component that is perpendicular to the cylinder, C_M and C_D are the inertia and drag coefficients respectively. In this study, the inertia and drag coefficients are obtained by the least square method based on the Morison equation and 15 successive cycles of sectional force at z=0. Figure 8 shows the comparison of the in-line force coefficient between attack angles. The in-line force coefficients agree with each other very well. The difference between them is less than 10% in the whole range of KC number examined.

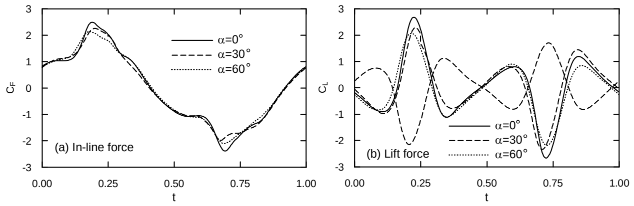

Figure 9. Mode averaged force coefficients for KC=17.5 and different oblique attack angles

Oscillatory flow past a circular cylinder for KC = 17.5 and at five different inclined angles (α =0, 15, 30, 45 and 60º) are simulated. It is observed that the vortex shedding flows at all the five inclined angles are in double pair regime. Figure 9 shows the comparison of non-dimensional force among α=0, 30, and 60º. The difference among the inline forces among the three α vales is very small. For α=30º, two flow patterns with one being the mirror image of the another are observed and the lift from both flow pattern are plotted in Figure 9 (b). It can be seen from Figure 9 (b) that there is little phase difference among the lift forces. However, the amplitude of the lift force varies a little bit with α. Figure 10 shows the variation of the inertia coefficient, drag coefficient, the maximum lift coefficient ($C_{L,max}$) and the root mean square value (RMS) of lift coefficient ($C_{L,rms}$) with the incline angle α for KC = 17.5. The coefficients $C_{L,max}$ and $C_{L,rms}$ are obtained according the mode averaged lift force for m = 3. The incline angle α has little effect on the in-line force coefficients C_M and C_D as shown in Figure 10. The $C_{L,max}$ also changes little if $\alpha \leq 45$º. The root mean square of the lift for α=60º is 12% smaller than that for α=0º. The maximum lift coefficient $C_{L,max}$ for α=60º is 20% smaller than that for α=0º.

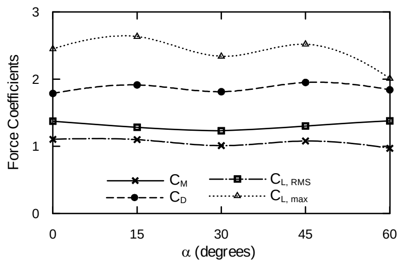

Figure 10. Variations of force coefficients with α (KC=17.5), the coefficients are based on the mode-averaged forces of mode m=3.

Conclusions

Oscillating flow around a circular at both right and oblique attack angles is investigated by solving the three-dimensional Navier-Stokes equations. Calculations are carried out for Reynolds number Re=2000 and KC number ranging from 6.75 to 30. The KC numbers examined cover four vortex shedding regimes: asymmetric, the transverse (single-pair), the diagonal (double-pair) and three-pair. The results are summarized below.

The one-pair, two-pair and three-pair flow regimes observed in the laboratory tests are identified by analysing the contour of the vorticity in the *xy*-plane.

Oscillatory flow past a circular cylinder at an oblique attack is simulated for $\alpha \leq 60°$. The flow regimes observed for flow with an oblique angle are very close to the right attack angle case. This is evidenced by the good agreement of the forces between cases with different attack angles. The flow regime mode does not change when attack angle increases from 0° to 60°. The helical span-wise streamlines are observed close to the cores of the span-wise vortex tubes. These vortices move with the vortex movement. The forces normalized by the velocity component normal to the cylinder agree exceptional well with the α=0° case. If the flow is in multi-modes, the mode-averaged force at each mode agrees with its counterpart at α=0° very well. The results show that the independence principle applies to the in-line force coefficients for $\alpha \leq 60°$. The results for KC = 17.5 shows that the maximum mode-averaged lift coefficient changes little when α increases from 0° to 45°, while it decreases by about 20% when α increases from 45° to 60°.

References

[1] Williamson, C.H.K., Sinusoidal flow relative to circular cylinders, *Journal of Fluid Mechanics*, 155, 1985, 141-174.

[2] Obasaju, E.D., Bearman, P.W. & Graham, J.M.R., A study of forces, circulation and vortex patterns around a circular cylinder in oscillatory flow, *Journal of Fluid Mechanics*, 196, 1988, 476-494.

[3] Lu, X.Y., Dalton, C. & Zhang, J.F., Application of large eddy simulation to an oscillating flow past a circular cylinder. *Journal of Fluids Engineering-Transactions of ASME*, 119 (3), 1997, 519-525.

[4] Zhang, J. & Dalton, C., The onset of three-dimensionality in an oscillating flow past a fixed circular cylinder. *Intl J. Numer. Meth. Fluids*, 30 (1), 1999, 19-42.

[5] Nehari, D., Armenio, V. & Ballio, F., Three-dimensional analysis of the unidirectional oscillatory flow around a circular cylinder at low Keulegan-Carpenter and b numbers, *Journal of Fluid Mechanics*, 520, 2004, 157-186.

[6] Ramberg, S., 1983. The effects of yaw and finite length upon the vortex wakes of stationary and vibrating circular cylinders. *Journal of Fluid Mechanics* 128, 81-107.

[7] Kozakiewicz, A., Fredsøe, J. & Sumer, B. M., 1995. Forces on pipelines in oblique attack: Steady current and waves, Proceedings of the 5 th International Offshore and Polar Engineering Conference, The Hague, The Netherlands, 2, 174-183.

[8] Thakur, A., Liu, X., Marshall, J. S., 2004. Wake flow of single and multiple yawed cylinders. *Journal of Fluids Engineering* 126, 861-870.

[9] Zhao, M., Cheng, L. & Zhou, T., 2009. Direction numerical simulation of three-dimensional flow past a yawed circular cylinder of infinite length. Journal of Fluids and Structures, accepted.

[10] Kozakiewicz, A., Fredsøe, J. & Sumer, B. M., Forces on pipelines in oblique attack: steady current and waves. *Proceeding of 5th International Offshore and Polar Engineering Conference, The Hague, The Netherlands*, 2, 1995, 174-18